iScience

CellPress
OPEN ACCESS

Article

IP_3-Dependent Ca^{2+} Oscillations Switch into a Dual Oscillator Mechanism in the Presence of PLC-Linked Hormones

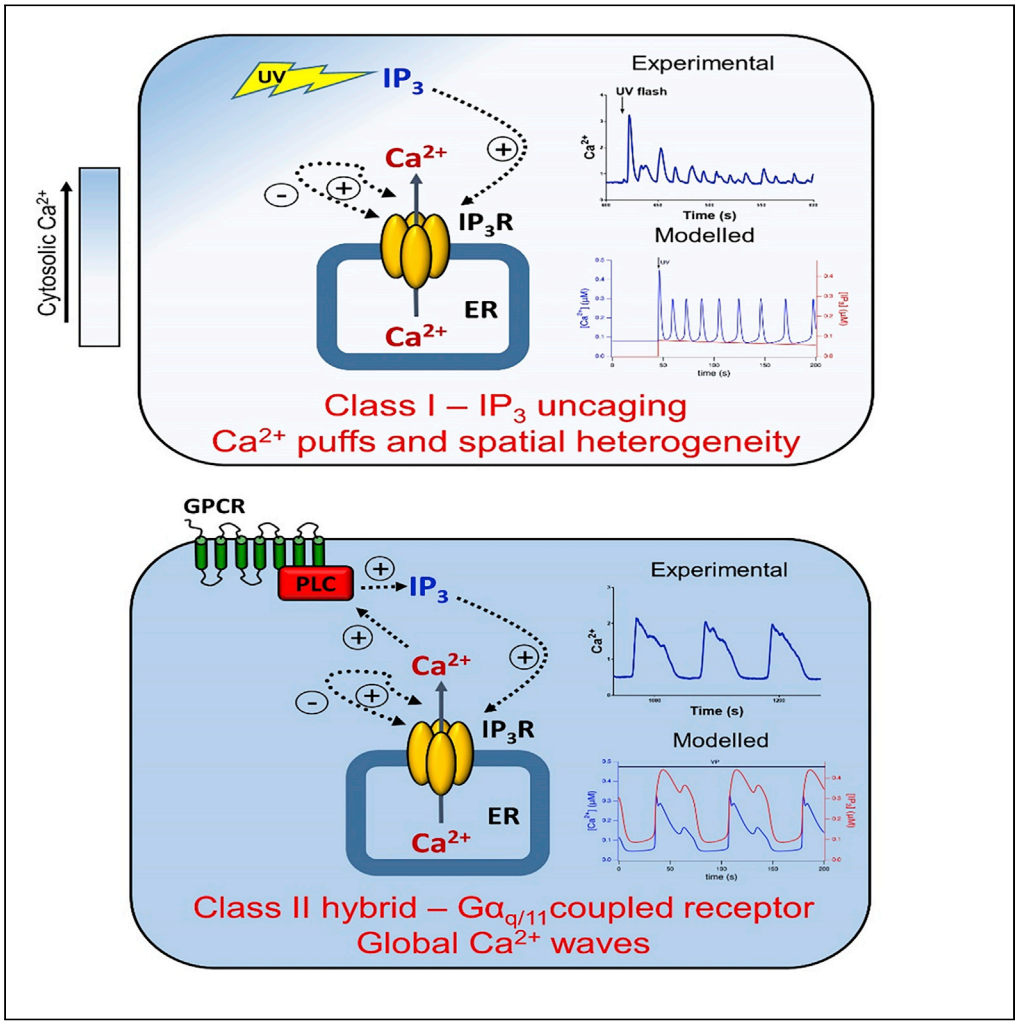

Paula J. Bartlett, Ielyaas Cloete, James Sneyd, Andrew P. Thomas

andrew.thomas@rutgers.edu

HIGHLIGHTS

Ca^{2+} oscillations driven by IP_3R (class 1) and PLC (class 2) occur in the same cell

IP_3 uncaging elicits brief and often spatially localized class 1 Ca^{2+} oscillations

GPCRs elicit whole-cell Ca^{2+} oscillations and waves via a hybrid class 2 mechanism

Dual Ca^{2+} feedback on IP_3R and PLC ensures a robust response to hormonal stimulation

Bartlett et al., iScience *23*, 101062
May 22, 2020
https://doi.org/10.1016/j.isci.2020.101062

iScience

CellPress
OPEN ACCESS

Article

IP_3-Dependent Ca^{2+} Oscillations Switch into a Dual Oscillator Mechanism in the Presence of PLC-Linked Hormones

Paula J. Bartlett,[1] Ielyaas Cloete,[2] James Sneyd,[2] and Andrew P. Thomas[1,3,*]

SUMMARY

Ca^{2+} oscillations that depend on inositol-1,4,5-trisphosphate (IP_3) have been ascribed to biphasic Ca^{2+} regulation of the IP_3 receptor (IP_3R) or feedback mechanisms controlling IP_3 levels in different cell types. IP_3 uncaging in hepatocytes elicits Ca^{2+} transients that are often localized at the subcellular level and increase in magnitude with stimulus strength. However, this does not reproduce the broad baseline-separated global Ca^{2+} oscillations elicited by vasopressin. Addition of hormone to cells activated by IP_3 uncaging initiates a qualitative transition from high-frequency spatially disorganized Ca^{2+} transients, to low-frequency, oscillatory Ca^{2+} waves that propagate throughout the cell. A mathematical model with dual coupled oscillators that integrates Ca^{2+}-induced Ca^{2+} release at the IP_3R and mutual feedback mechanisms of cross-coupling between Ca^{2+} and IP_3 reproduces this behavior. Thus, multiple Ca^{2+} oscillation modes can coexist in the same cell, and hormonal stimulation can switch from the simpler to the more complex to yield robust signaling.

INTRODUCTION

Oscillations of intracellular Ca^{2+} represents a fundamental cellular signaling mechanism regulating a multitude of process such as fertilization, metabolism, and secretion (Rooney et al., 1989; Bootman et al., 1997b; Berridge et al., 2000; Berridge, 2016). In non-excitable cells, oscillations of cytosolic Ca^{2+} ($[Ca^{2+}]_c$) are generated by activation of hormone receptors coupled to phospholipase C (PLC) that produce the second messenger inositol-1,4,5-trisphosphate (IP_3), which activates IP_3 receptor Ca^{2+} release channels (IP_3R) in the endoplasmic reticulum (ER). The Ca^{2+} signaling toolkit of channels, pumps, and regulatory proteins is well defined (Berridge et al., 2000; Berridge, 2017), but the mechanisms driving cyclical changes in $[Ca^{2+}]_c$ have yet to be resolved. In hepatocytes, several IP_3-dependent hormones regulate metabolism and a number of other functions via baseline-separated $[Ca^{2+}]_c$ oscillations. Hepatocytes exhibit frequency modulation, whereby the $[Ca^{2+}]_c$ oscillation frequency is determined by agonist concentration, but the individual Ca^{2+} spikes have constant amplitude and rate of rise, and propagate as intracellular $[Ca^{2+}]_c$ waves at a constant velocity, independent of agonist dose (Rooney et al., 1989; Thomas et al., 1991; Gaspers and Thomas, 2005; Bartlett et al., 2014). Moreover, these hormone-induced Ca^{2+} transients are an all-or-none phenomenon, whereby the Ca^{2+} waves propagate at full strength across the whole cell. In the intact liver, Ca^{2+} waves propagate from cell to cell through gap junctions, and hence across the entire liver lobules to regulate hepatic metabolism and glucose output (Gaspers et al., 2019). We propose that Ca^{2+}-dependent activation of PLC provides a feedforward mechanism to elicit robust cell-wide Ca^{2+} increases throughout the cytoplasm, ensuring maximal activation of Ca^{2+}-dependent processes. Alterations in Ca^{2+} homeostasis and signaling have been shown in diseases of the liver (Bartlett et al., 2017; Arruda and Hotamisligil, 2015), therefore elucidating the mechanisms that maintain Ca^{2+} oscillations is critical to understanding Ca^{2+} dysregulation in disease states such as fatty liver disease and diabetes.

Experimental and mathematical modeling studies have explored the $[Ca^{2+}]_c$ oscillatory phenomenon without reaching a consensus in terms of mechanism. Two distinct hypotheses have been proposed: class 1 oscillations, which arise solely due to the biphasic effects Ca^{2+} on IP_3R gating (Bezprozvanny et al., 1991; Thurley and Falcke, 2011; De Young and Keizer, 1992; Marchant and Parker, 2001) and rely only on a continuous elevation of IP_3, and class 2 oscillations, which rely on Ca^{2+} feedback regulation of IP_3 levels such that $[Ca^{2+}]_c$ oscillations are coupled to, and dependent on, IP_3 oscillations (Politi et al., 2006; Salazar et al., 2008;

[1]Department of Pharmacology, Physiology and Neuroscience, New Jersey Medical School Rutgers, The State University of New Jersey, Newark, NJ 07103, USA

[2]Department of Mathematics, The University of Auckland, Auckland, New Zealand

[3]Lead Contact

*Correspondence: andrew.thomas@rutgers.edu

https://doi.org/10.1016/j.isci.2020.101062

Dupont and Erneux, 1997). Currently, cells are classified into class 1 Ca^{2+}-induced Ca^{2+} release (CICR) or class 2 IP_3 dynamics-dependent Ca^{2+} oscillators. Experimental evidence from different cell types is used to support each of the two models, and thus the discrepant findings may reflect differences in the cellular complement and subcellular distributions of the Ca^{2+} signaling toolkit components.

Mathematical models based on biphasic regulation of the IP_3R by Ca^{2+}, effectively IP_3-dependent CICR, yield Ca^{2+} oscillations with a high frequency and a narrow sensitivity to PLC activity and IP_3 concentration (Bezprozvanny et al., 1991; De Young and Keizer, 1992; Sneyd et al., 2017; Thurley and Falcke, 2011). This is borne out by the nature of the $[Ca^{2+}]_c$ signals observed in cell types where experimental evidence indicates that class 1 Ca^{2+} oscillations occur. Hepatocytes and many other secretory cells generate $[Ca^{2+}]_c$ oscillations with long interspike intervals (ISIs) and kinetics that are independent of agonist dose, which cannot be readily reproduced by class 1 oscillatory models. The long periods at basal $[Ca^{2+}]_c$ between Ca^{2+} transients at low hormone doses, together with a broad dynamic range of frequency modulation, suggests that these $[Ca^{2+}]_c$ oscillations are controlled by other feedback loops such as those that regulate IP_3 generation and metabolism (Meyer and Stryer, 1988; Politi et al., 2006; Gaspers et al., 2014; Kummer et al., 2000). In the hepatocyte modeling studies of Kummer et al. (Kummer et al., 2000), an autocatalytic activity of the G_α subunit of the G-protein drives dynamic PLC activation and hence IP_3 oscillations, with Ca^{2+} causing negative feedback on PLC. However, these activities have not been reported experimentally, and although their model reproduces baseline spiking, it also leads to chaotic behavior that is not usually observed in our studies. In general, models that rely on Ca^{2+}-dependent IP_3 degradation or feedback inhibition of PLC activity do not fully reproduce the types of $[Ca^{2+}]_c$ oscillations generated by G-protein-coupled receptor (GPCR)-linked hormones in hepatocytes (Gaspers et al., 2014; Dupont et al., 2003). By contrast, class 2 mathematical models incorporating positive Ca^{2+} feedback on IP_3 formation can reproduce the $[Ca^{2+}]_c$ oscillatory patterns observed in these cells (Gaspers et al., 2014; Meyer and Stryer, 1988; Politi et al., 2006). In most models involving positive Ca^{2+} feedback on IP_3 formation, a component of Ca^{2+} activation of the IP_3R is also generally required to reproduce the observed waveform of baseline-separated $[Ca^{2+}]_c$ oscillations with a rapidly rising phase (Politi et al., 2006; Gaspers et al., 2014), making the relevant class 2 models a hybrid of class 2 and class 1 properties.

Our previous work has demonstrated that expression of a recombinant IP_3 buffer in hepatocytes slows or completely eliminates (at high expression levels) hormone-induced $[Ca^{2+}]_c$ oscillations and waves (Gaspers et al., 2014). These data, combined with mathematical modeling of the predicted effects of an IP_3 buffer, argue that a periodic rapid rise in IP_3 via Ca^{2+} feedforward activation of PLC is essential for generating $[Ca^{2+}]_c$ oscillations in hepatocytes. Previously, we showed that PLC inhibition does not affect $[Ca^{2+}]_c$ oscillations generated by IP_3 uncaging in hepatocytes, indicating that agonist-dependent activation of PLC is a prerequisite for the feedforward regulation seen with hormonal stimulation (Bartlett et al., 2015). Furthermore, we identified both positive and negative feedback regulation of Ca^{2+} oscillations by protein kinase C (PKC), at least part of which is due to inhibition of GPCR-dependent PLC activation. It is possible that this could underlie the unique and distinctively reproducible Ca^{2+} spike shapes elicited by activation of different GPCRs in hepatocytes (Rooney et al., 1989).

Subcellular Ca^{2+} blips and puffs are local events that can recruit other Ca^{2+} release sites to summate into global $[Ca^{2+}]_c$ oscillations and propagate as saltatory $[Ca^{2+}]_c$ waves (Bootman et al., 1997a; Bootman and Berridge, 1995). Intracellular uncaging of IP_3 has been employed as a tool to mimic hormone-induced Ca^{2+} responses and interrogate the basic parameters of localized and global Ca^{2+} release events (Marchant et al., 1999; Marchant and Parker, 2001; Smith et al., 2009; Lock et al., 2017). The local Ca^{2+} signals generated by uncaging IP_3 can provide information about the sensitivity of a given cell to IP_3 and the speed and extent of CICR via the resident Ca^{2+} release channels. Moreover, CICR at the level of IP_3R channels is sufficient to drive $[Ca^{2+}]_c$ oscillations and Ca^{2+} wave propagation. However, IP_3 uncaging does not recapitulate the $[Ca^{2+}]_c$ responses to physiological hormonal stimuli in hepatocytes.

The current consensus is that cells exhibit either class 1 or class 2 Ca^{2+} oscillations and that these occur unambiguously (Sneyd et al., 2006, 2017). However, the present data obtained in hepatocytes suggest that these mechanisms are not mutually exclusive. Photorelease of IP_3 alone elicits high-frequency $[Ca^{2+}]_c$ oscillations with an amplitude, width, and rate of rise that increase with stimulus strength. These responses can be observed in local Ca^{2+} puff sites or globally across the cell, and importantly, they are not perturbed by the expression of an intracellular IP_3 buffer. We conclude that these are CICR-dependent

$[Ca^{2+}]_c$ oscillations. However, there is a dramatic shift in the oscillatory pattern upon the addition of a hormone to cells responding to flash photolysis of caged IP_3. The $[Ca^{2+}]_c$ oscillations in the presence of vasopressin (VP) become much broader, with a prolonged ISI, a very regular frequency, and manifesting as Ca^{2+} waves that consistently propagate through the entire cell. A mathematical model incorporating both CICR at the IP_3R and hormone-dependent Ca^{2+} feedback on IP_3 generation faithfully reproduces both modes of $[Ca^{2+}]_c$ oscillations and the ability to transition between them. These data show that class 1 and class 2 $[Ca^{2+}]_c$ oscillations can coexist in the same cell and demonstrate that hormone-dependent $[Ca^{2+}]_c$ oscillations require dual feedback loops that dynamically control Ca^{2+} release and IP_3 levels during the oscillation cycle. Importantly, class 2 oscillations dominate over class 1 in the presence of hormone.

RESULTS

Graded $[Ca^{2+}]_c$ Responses to Flash Photolysis of Caged IP_3

The genetically encoded Ca^{2+} indicators GCaMP3 and RGECO-1 were used to detect $[Ca^{2+}]_c$ responses elicited by IP_3 uncaging and activation of the PLC-coupled VP receptor (V1R). Expression of molecular Ca^{2+} indicators offers a number of advantages over chemical indicators such as fluo4. The apparent affinities for Ca^{2+} of GCaMP3 and RGECO1 (405 and 449 nM, respectively; Akerboom et al., 2013) are comparable with that of fluo4 (335 nM), but they have a higher quantum yield and are typically expressed at a lower effective concentration. They are also less diffusible and so are less likely to perturb local Ca^{2+} dynamics. It is also an advantage that they have an exclusive cytosolic location (unlike the chemical indicators, which also load into subcellular compartments). Empirically, we find that these genetically encoded Ca^{2+} indicators are well suited to the resolution of small and local $[Ca^{2+}]_c$ signals. In the present study, we analyzed the local, global, and propagating properties of $[Ca^{2+}]_c$ oscillations elicited by global IP_3 uncaging and VP treatment, with a view to dissecting the mechanisms driving baseline-separated $[Ca^{2+}]_c$ oscillations.

Hormonal regulation of metabolism in hepatocytes has been extensively characterized by our group, and we have shown that $[Ca^{2+}]_c$ oscillation frequency, rather than amplitude, encodes signal strength (Bartlett et al., 2014; Gaspers and Thomas, 2005; Rooney et al., 1989; Thomas and Robb-Gaspers, 1996). Different GPCRs give rise to $[Ca^{2+}]_c$ oscillations with distinct Ca^{2+} spike shapes, reflected primarily in the rate of decay of each Ca^{2+} spike, and this too is independent of agonist dose. By contrast, photorelease of caged IP_3 in GCaMP3-expressing hepatocytes induced $[Ca^{2+}]_c$ oscillations whose amplitude and duration increased in a dose-dependent manner (Figure 1A; see also Transparent Methods). Analysis of global (whole-cell) $[Ca^{2+}]_c$ responses showed that as the number of UV pulses was increased, the $[Ca^{2+}]_c$ peak height, peak width (measured as full width at half maximum; FWHM), rate of rise, and frequency increased, and there was a concomitant decrease in ISI (Figures 1B–1E). For each of these experiments, 5 nM VP was also added. VP-induced $[Ca^{2+}]_c$ oscillations had amplitudes and rates of Ca^{2+} rise that were similar to the maximum response to IP_3 uncaging, whereas the $[Ca^{2+}]_c$ peak widths and ISI were much longer than was observed with IP_3 uncaging.

We have previously demonstrated that hormone-induced Ca^{2+} oscillations are inhibited by the PLC inhibitor U73122, whereas oscillations induced by photorelease of caged IP_3 are insensitive to PLC inhibition (Bartlett et al., 2015). Thus, without GPCR activation the mechanisms required to drive regenerative IP_3 increases are lacking. Furthermore, in contrast to the sustained hormone-induced $[Ca^{2+}]_c$ oscillations, the responses elicited by caged IP_3 run down, as shown by the decrease in Ca^{2+} transient amplitude (Figure 1A). Taken together, these data demonstrate that an increase in IP_3 alone does not recapitulate the effect of GPCR activation.

Continuous Uncaging of IP_3

Caged IP_3 can also be photolyzed slowly using a xeon light source and UV illumination over a prolonged period (as opposed to the discrete UV laser flashes reported in the previous section) to more closely mimic the continuous generation of IP_3 during hormonal stimulation. In the majority of cells (72% $\pm$ 6%, mean $\pm$ SEM, 45 cells from 3 independent experiments), continuous IP_3 uncaging resulted in a slow monophasic rise in $[Ca^{2+}]_c$ throughout the cell, but $[Ca^{2+}]_c$ oscillations were also observed in ~25% cells (Figures S1A and S1B). Similar to the observations with flash photolysis of caged IP_3, these $[Ca^{2+}]_c$ oscillations had a higher frequency and shorter spike duration than hormone-induced oscillations, whereas the rate of $[Ca^{2+}]_c$ rise was the same (Figures S1C and S1D). We have previously shown that expression of the ligand-binding domain of rat IP_3R type 1 (LBD) acts as an intracellular IP_3 buffer, which slows hormone-induced $[Ca^{2+}]_c$ oscillations and waves in primary hepatocytes (Gaspers et al., 2014). In that study we

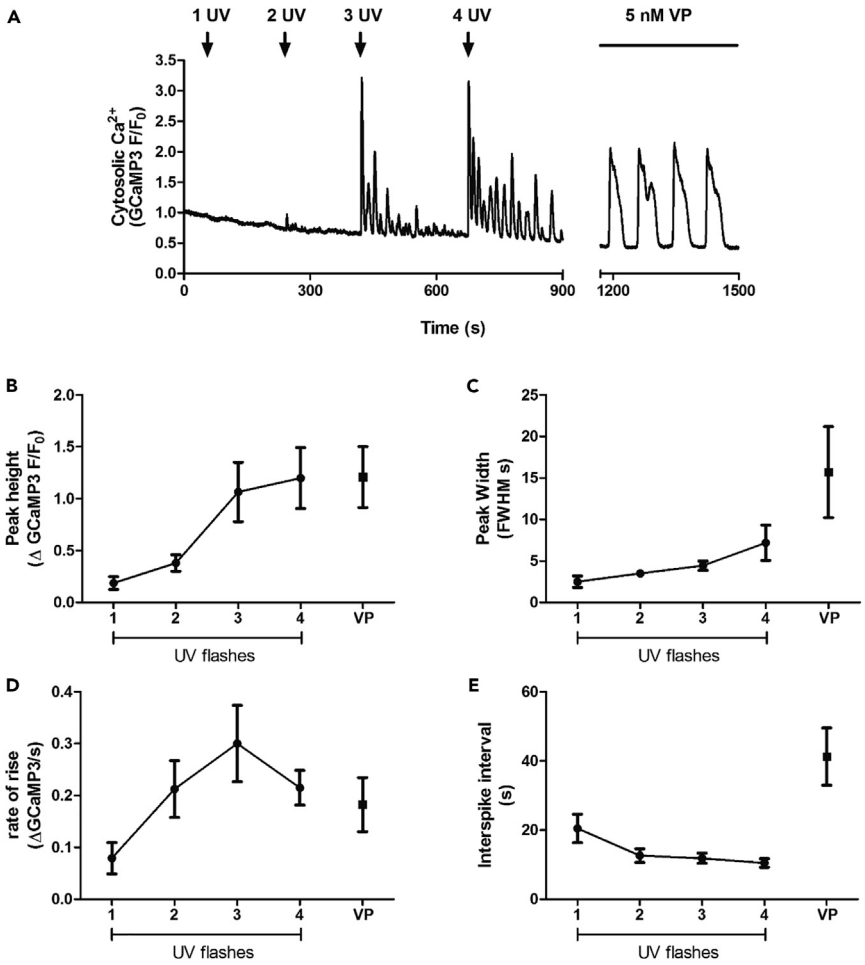

Figure 1. Effect of Incremental Flash Photolysis of Caged IP_3 on $[Ca^{2+}]_c$ Oscillation Properties

Isolated hepatocytes were transfected with GCaMP3, cultured overnight, and then loaded with caged IP_3 (2 μM; 1 h).

(A) Representative trace showing cytosolic Ca^{2+} responses to photolysis of caged IP_3 elicited by rapid trains of 1, 2, 3, and 4 UV pulses (arrows). After a recovery period, the same cells were stimulated with 5 nM vasopressin (VP).

(B–E) Summary data for the effect of increasing UV stimulation compared with VP for $[Ca^{2+}]_c$ spike amplitude (B), peak width measured as full width at half maximum (FWHM) (C), rate of rise (D), and interspike interval (ISI) (E). Data are mean ± SEM of the second $[Ca^{2+}]$ transient for amplitude, width, and rate of rise, and 3 consecutive oscillations for ISI after UV pulse or 5 nM VP addition (11 cells from 6 independent experiments).

showed that LBD expression did not affect the rate of rise or amplitude of the slow monophasic $[Ca^{2+}]_c$ response to continuous IP_3 uncaging. As shown in Figure 2, LBD expression also had no effect on the peak width, ISI, or rate of rise of the oscillatory $[Ca^{2+}]_c$ responses generated by slow uncaging of IP_3. Thus, in the absence of hormone, when IP_3 reaches the threshold for CICR-mediated $[Ca^{2+}]_c$ oscillations the kinetic properties of these oscillations is unaffected by the presence of an IP_3 buffer, as predicted for a class 1 model.

Subcellular Organization of Ca^{2+} Signals Elicited by Global Flash Photolysis of Caged IP_3

The preceding data describe only the integrated whole-cell $[Ca^{2+}]_c$ events elicited by IP_3 uncaging, but IP_3 uncaging can also cause localized subcellular Ca^{2+} release. Local Ca^{2+} release responses termed Ca^{2+} puffs have been observed in *Xenopus* oocytes after photorelease of caged IP_3 (Marchant and Parker, 2001), and similar localized Ca^{2+} release events have also been reported in mammalian cell lines (Smith et al., 2009; Thomas et al., 2000; Tovey et al., 2001). Local Ca^{2+} release events have not previously been reported in hepatocytes in response to photorelease of caged IP_3 (Bartlett et al., 2015; Gaspers et al., 2014) or following hormone stimulation (Rooney et al., 1990; Thomas et al., 1996). In the present study, the use of a genetically encoded Ca^{2+}

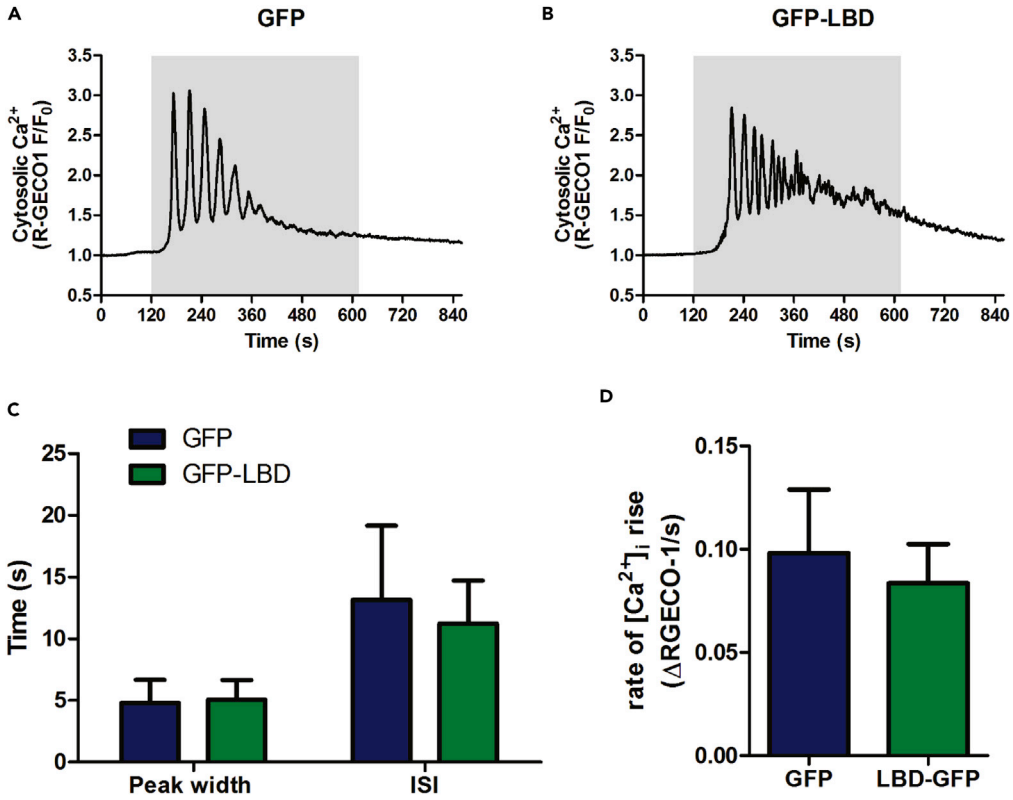

Figure 2. Buffering of Intracellular IP_3 Has No Effect on Ca^{2+} Oscillations Elicited by Slow Release of Caged IP_3

(A–D) Hepatocytes cotransfected with RGECO1 and either GFP (A) or GFP-LBD (B) were loaded with caged IP_3 (2 μM; 1 h). The gray area shows the duration of slow IP_3 uncaging elicited by low-intensity UV illumination (50-ms exposures from xenon lamp at 2 Hz). Expression of GFP-LBD had no effect on the peak width (FWHM) or ISI (C) or the rate of Ca^{2+} rise (D). Data are mean ± SEM of 10 cells from 4 independent experiments.

indicator that has less effect on Ca^{2+} diffusion and buffering than small molecule chemical indicator dyes has revealed spatial heterogeneity in the $[Ca^{2+}]_c$ responses to submaximal levels of photoreleased IP_3. As shown in Figure 3, low levels of IP_3, particularly in the threshold range elicited by 1 or 2 UV pulses, caused localized $[Ca^{2+}]_c$ transients at discreet subcellular locations in ~40% cells (23 of 59 cells, 6 independent experiments). In the other cells analyzed, where the initial IP_3 uncaging presumably exceeded this threshold, oscillatory propagating Ca^{2+} waves or a single global $[Ca^{2+}]_c$ response were observed (summarized in Figure 3E). Importantly, the data of Figure 3E show a progression from predominantly local events, to propagating oscillations, to global $[Ca^{2+}]_c$ elevations as the UV flash density was increased.

The localized Ca^{2+} release events observed with IP_3 uncaging in hepatocytes (Figure 3A) were 3.3 ± 0.3 μm in diameter (mean ± SEM, n = 23 cells from 6 independent experiments), which is similar to the Ca^{2+} puffs reported in other cell types, including *Xenopus* oocytes (Marchant and Parker, 2001; Tovey et al., 2001; Thomas et al., 2000). We therefore refer to the localized hepatocyte Ca^{2+} transients in the present study as Ca^{2+} puffs, although they differ somewhat from most previous reports in having a longer duration. Another difference from previous reports of Ca^{2+} puffs elicited by IP_3 is that they typically occurred at a single repeating location at the cell periphery in the primary cultured hepatocyte (87% of cells). Significantly, these "eager" Ca^{2+} release sites corresponded to the site of Ca^{2+} wave initiation by hormones in the same cell. This polarization may reflect the reported subcellular distribution of IP_3 receptors in hepatocytes, with the more sensitive type 2 IP_3R predominantly in the apical region where hormone-induced Ca^{2+} waves originate and type 1 IP_3R uniformly distributed across the cell (Hernandez et al., 2007; Nagata et al., 2007). In cells with a diffuse distribution of IP_3Rs, Ca^{2+} puffs occur in multiple locations, although there are still discrete eager sites (Smith et al., 2009; Tovey et al., 2001; Marchant and Parker, 2001). Thus, the functional polarization of the hepatocyte allows for a stable Ca^{2+} release site that presumably engages multiple IP_3R clusters to form a discrete integrated Ca^{2+} puff site.

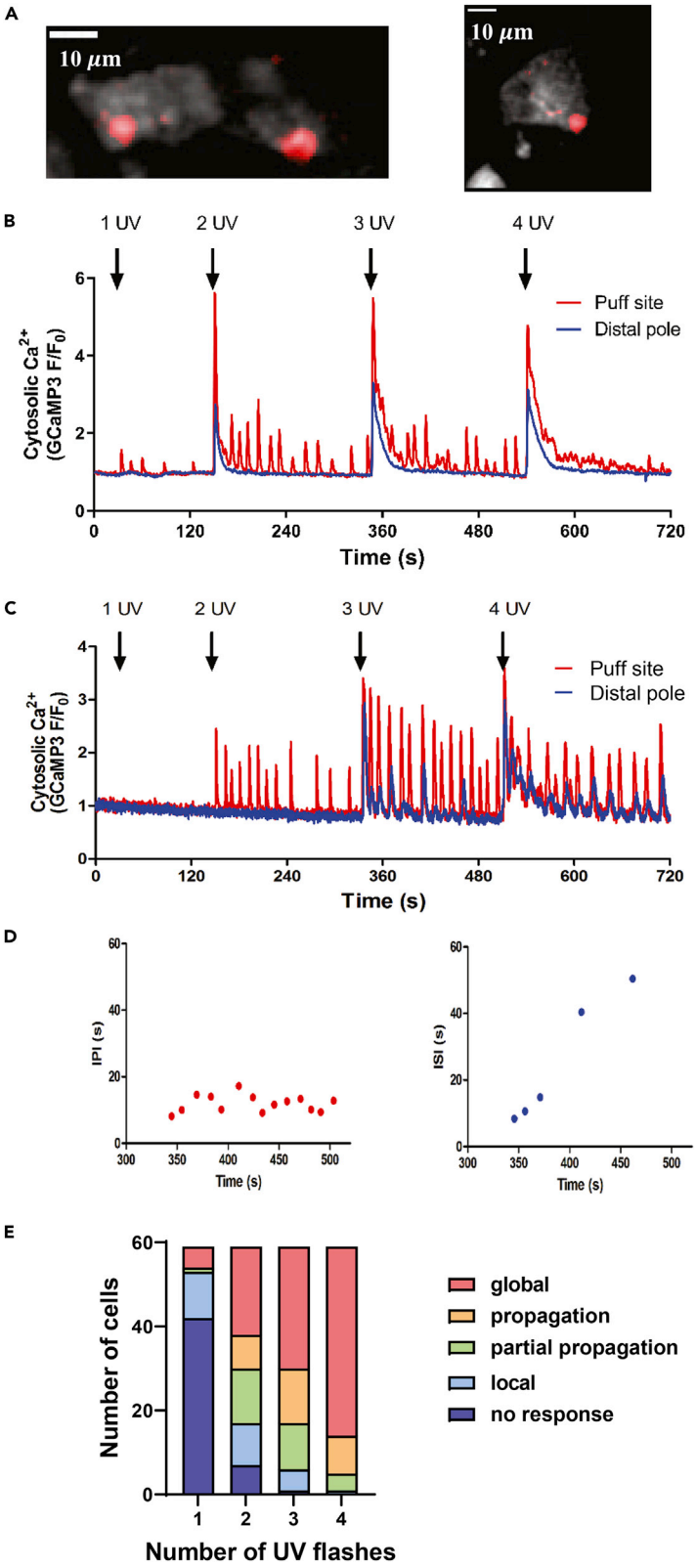
A
10 μm
10 μm
B
1 UV
2 UV
3 UV
4 UV
Puff site
Distal pole
Cytosolic Ca2+ (GCaMP3 F/F0)
Time (s)
C
1 UV
2 UV
3 UV
4 UV
Puff site
Distal pole
Cytosolic Ca2+ (GCaMP3 F/F0)
Time (s)
D
IPI (s)
Time (s)
ISI (s)
Time (s)
E
Number of cells
Number of UV flashes
global
propagation
partial propagation
local
no response

Figure 3. Spatial Properties of $[Ca^{2+}]_c$ Responses Elicited by Flash Photolysis of caged IP_3

Isolated hepatocytes were transfected with GCaMP3, cultured overnight, and then loaded with caged IP_3 (2 μM; 1 h).
(A) Single video frames showing focal $[Ca^{2+}]_c$ release events. Scale bar, 10 μM.
(B and C) Representative traces of changes in $[Ca^{2+}]_c$ at the local puff site (red) and distal pole (blue) of two individual hepatocytes during IP_3 uncaging.
(D) Interpuff interval (IPI, red) and interspike interval (ISI, blue) during the 3 UV pulse response from (C).
(E) Ordinal plot of the Ca^{2+} response pattern for cells with increasing UV pulse density (bursts of 1–4 flashes, as indicated). Response patterns of increasing strength are classified as follows: *no response*, *local* Ca^{2+} transients at a discrete puff site, *partial propagation* where Ca^{2+} waves only propagated across the cell intermittently, *propagation* where Ca^{2+} waves consistently propagated across the cell, and *global* for whole-cell Ca^{2+} responses that were not spatially resolved (summary of 59 cells from 6 independent experiments).

To characterize the local and global Ca^{2+} events in each cell, $[Ca^{2+}]_c$ in the region of interest at the Ca^{2+} puff site and at the distal pole of the cell were analyzed. Figures 3B and 3C show example Ca^{2+} traces from two cells with the puff site and distal pole superimposed. In these studies the $[Ca^{2+}]_c$ signals at the distal region reflect the propagation of Ca^{2+} waves from the puff site (Rooney et al., 1990; Gaspers et al., 2019; Gaspers and Thomas, 2005). We have determined the frequency of oscillations at each site from the interval between Ca^{2+} transients; by convention the term *inter-puff interval* (IPI) is used for events at the Ca^{2+} puff site and *inter-spike interval* (ISI) for events that propagate across the whole cell. Submaximal levels of IP_3 uncaging frequently generated localized Ca^{2+} oscillations at the puff site that did not propagate across the whole cell, as shown in Figure 3B, 1 UV flash, and Figure 3C, 2 UV flashes. As the stimulus strength was increased (number of UV flashes), $[Ca^{2+}]_c$ waves were observed to propagate across the cell, radiating from the puff site. However, the effect of IP_3 uncaging on Ca^{2+} responses at the distal pole of the cell did not always mirror the Ca^{2+} oscillations at the puff site. In some cases only the first Ca^{2+} transient at the puff site propagated across the cell as a single Ca^{2+} wave (Figure 3B). When multiple Ca^{2+} transients at the puff site did propagate as Ca^{2+} waves they often declined in amplitude. Importantly, not all $[Ca^{2+}]_c$ transients at the puff site were transmitted across the hepatocyte to the distal pole (Figure 3C). This failure to propagate manifests in the difference in IPI and ISI plotted in Figure 3D for the 3 UV uncaging response in Figure 3C (see also Figure 5E). The continuum of increasingly effective propagation with increasing UV flash density is summarized in Figure 3E.

In contrast to IP_3 uncaging, stimulation with a PLC-linked hormone such as VP leads to Ca^{2+} oscillations that consistently propagate across the entire cell throughout the active dose range, with the characteristic long-duration $[Ca^{2+}]_c$ spikes described earlier (Figures 1 and S2; Gaspers and Thomas, 2005; Bartlett et al., 2014; Rooney et al., 1990). Moreover, low concentrations of hormone cause baseline-separated broad $[Ca^{2+}]_c$ oscillations with long 1- to 5-min ISIs. We attempted to mimic this behavior by eliciting periodic IP_3 uncaging with a similar frequency using single UV flash events (Figure S3). However, this did not reproduce the typical whole-cell baseline-separated Ca^{2+} oscillations observed with hormone. Instead multiple local Ca^{2+} transients were observed with the initial UV flashes. Although these did propagate to the distal pole as more IP_3 was released into the hepatocyte, the $[Ca^{2+}]_c$ spikes elicited by periodic uncaging never took on the broad profile of those observed with VP.

Effect of IP_3 Uncaging during Hormone-Induced $[Ca^{2+}]_c$ Oscillations

Photolysis of caged IP_3 during a train of hormone-induced $[Ca^{2+}]_c$ oscillations has been explored as an approach to determine whether receptor-mediated $[Ca^{2+}]_c$ oscillations are dependent on oscillating or steady-state IP_3 levels (Sneyd et al., 2006, 2017). Mathematical modeling predicts that class 1 oscillating cells show an increase in frequency following a pulse of IP_3, and this has been demonstrated experimentally (Sneyd et al., 2006). For class 2 oscillating cells it has been predicted that an increase in $[IP_3]$ will result in a delay before Ca^{2+} oscillations recommence, because the IP_3 level needs to fall before a subsequent Ca^{2+} spike can be initiated (Sneyd et al., 2006).

In hepatocytes, photolysis of caged IP_3 during a train of VP-induced $[Ca^{2+}]_c$ oscillations either slightly reduced the Ca^{2+} oscillation frequency (Figure 4A, 22/32 cells) or in some cases led to a temporary arrest of oscillations, as predicted from class 2 models (Figure 4B, 7/32 cells). In cells where the global hormone-induced $[Ca^{2+}]_c$ oscillations were arrested, small local $[Ca^{2+}]_c$ puffs were often observed during the interruption in the whole-cell $[Ca^{2+}]_c$ oscillations. The decrease in oscillation frequency observed in the majority of cells is shown in Figure 4C, with mean pre- and post-photolysis values of 0.76 ± 0.07 min^{-1} and 0.59 ± 0.09 min^{-1}, respectively (mean ± SEM for 32 hepatocytes from 4 independent experiments; 5 min pre- and post-UV; $p < 0.001$ by paired Student's t test). When the same UV pulse protocol was applied to VP-stimulated hepatocytes not loaded with caged IP_3, the pre- and post-flash values were

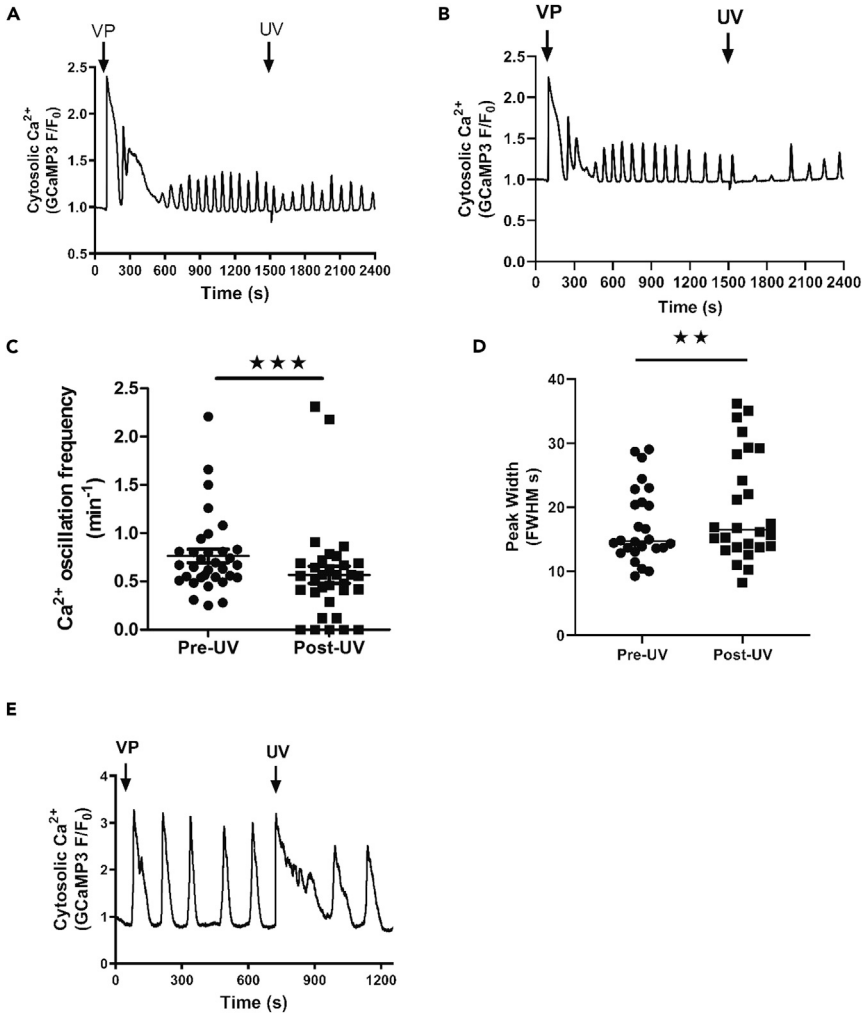

Figure 4. Effect of IP_3 Uncaging on $[Ca^{2+}]_c$ Responses Elicited by Vasopressin

(A–D) Isolated hepatocytes were transfected with GCaMP3, cultured overnight and then loaded with caged IP_3 (2 μM; 1h). Hepatocytes were stimulated with vasopressin (VP) and then IP_3 uncaging was achieved by a brief (1-s) pulse of 340-nm light from the microscope fluorescence illuminator Xeon lamp. Representative traces showing (A) a slight slowing of Ca^{2+} oscillation frequency or (B) the temporary arrest of oscillations. Summary data showing a decrease in oscillation frequency (C) and an increase in peak width (D) after the IP_3 uncaging event (data are mean ± SEM from ≥26 individual hepatocytes from 4 independent experiments, **$p < 0.01$, ***$p < 0.001$ paired Student's t test).

(E) Representative trace of hepatocyte stimulated with VP and then IP_3 uncaging with 3 UV flashes from UV laser.

0.84 ± 0.07 min^{-1} and 0.77 ± 0.09 min^{-1}, respectively (15 cells from 2 independent experiments; $p = 0.15$). The decrease in frequency following IP_3 uncaging was associated with an increase in Ca^{2+} transient width from 17.1 ± 1.1 s to 19.8 ± 1.6 s FWHM (Figure 4D; mean ± SEM for 26 hepatocytes from 4 independent experiments; $p < 0.01$ by paired Student's t test). As shown in Figure 4E, stronger IP_3 uncaging (3 UV laser pluses) during a train of VP-induced $[Ca^{2+}]_c$ oscillations caused a more pronounced prolongation of the $[Ca^{2+}]_c$ spikes, but did not increase the oscillation frequency as would be expected for a class 1 mechanism. Presumably under the conditions of Figure 4E the uncaged IP_3 extends the time required for IP_3 levels to decay and hence delays Ca^{2+} refilling of the ER. Taken together, the data of Figure 4 are consistent with the hypothesis that hormones elicit predominantly class 2 $[Ca^{2+}]_c$ oscillations that depend on fluctuations of IP_3 in hepatocytes, because an increase in $[IP_3]$ did not translate to an increase in oscillation frequency.

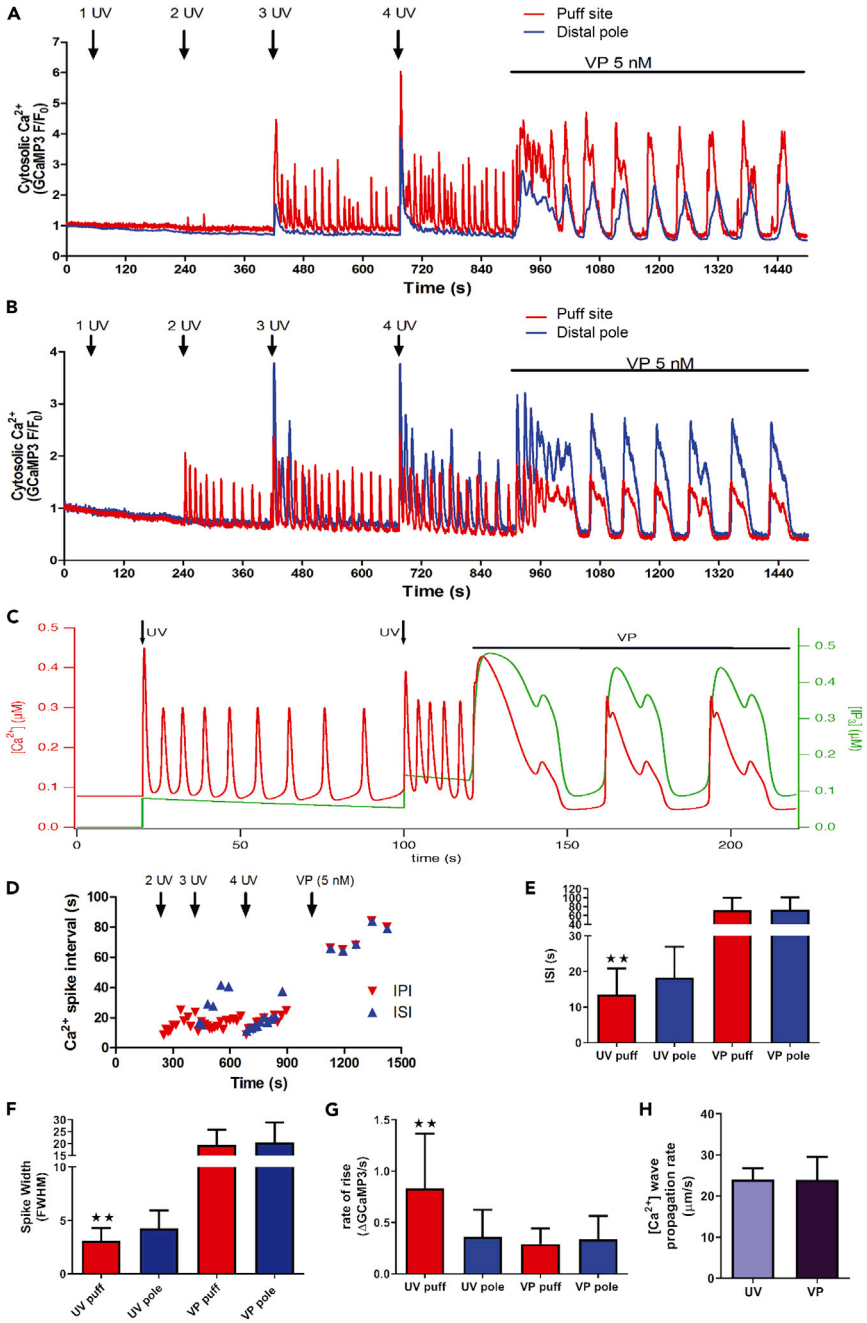

Figure 5. Fast $[Ca^{2+}]_c$ Oscillations Elicited by IP_3 Uncaging Transition to Broad Baseline-Separate $[Ca^{2+}]_c$ Oscillations in the Presence of Hormone

Isolated hepatocytes were transfected with GCaMP3, cultured overnight, and then loaded with caged IP_3 (2 μM; 1 h). Rapid trains of 1, 2, 3, or 4 UV pulses were applied as indicated (arrows) followed by the addition of VP (5 nM).

(A and B) Representative traces showing cytosolic $[Ca^{2+}]_c$ oscillations at puff site (red) and distal pole (blue) of two cells in response to IP_3 uncaging and VP (see also Videos S1 and S2).

(C) Mathematical model combining class 1 and class 2 oscillation mechanisms predicts the observed behavior in this paradigm (red line $[Ca^{2+}]_c$, green line $[IP_3]$).

(D) IPI and ISI of cell shown in (B) in response to UV pulses and VP (transition period between UV and VP responses not shown).

(E–G) Comparison of ISI (E), spike width (FWHM) (F), and rate of rise (G) at the puff site and distal pole of hepatocytes.

Figure 5. *Continued*
(H) Comparison of $[Ca^{2+}]_c$ wave propagation rate elicited by UV and VP. Data are mean ± SEM of 10 cells from 5 independent experiments. **p < 0.01, paired Student's t test.

Addition of hormone during IP_3-induced $[Ca^{2+}]_c$oscillations causes a qualitative shift in Ca^{2+} oscillation properties

Our previous work (Bartlett et al., 2015) and data presented in the current study, demonstrate that release of IP_3 alone is incapable of reproducing oscillatory $[Ca^{2+}]_c$ transients with the same properties as those observed with hormone stimulation. To further test the hypothesis that baseline-separated Ca^{2+} oscillations depend on cross-coupling of IP_3 and Ca^{2+} we reversed the paradigm of Figure 4 and examined the effect of adding VP during a train of oscillations induced by IP_3 uncaging. Flash photolysis events were incrementally increased, and then VP was added while cells were still responding to the uncaged IP_3. The $[Ca^{2+}]_c$ signals in puff sites and at the distal pole of the cell were then compared between uncaging and hormone-induced responses. Strikingly, the application of VP resulted in a dramatic shift in oscillatory behavior from high-frequency, small-width oscillations, only some of which propagated across the whole cell (as summarized in Figure 3E), to lower-frequency broad $[Ca^{2+}]_c$ oscillations that always engaged the entire cell (Figures 5A and 5B; see also Videos S1 and S2). The IPI and ISI for the cell shown in Figure 5B are plotted in Figure 5D. These data show reliable and complete propagation of the hormone-induced $[Ca^{2+}]_c$ oscillations throughout the cell, whereas the higher-frequency $[Ca^{2+}]_c$ transients with IP_3 uncaging were irregular and inconsistent in engaging the distal pole of the cell. Videos S1 and S2 show this cell (in center) and other cells that exhibit similar behavior. Video S1 shows the changes in $[Ca^{2+}]_c$ in response to UV flash events and then subsequent VP addition; increases in GCaMP3 fluorescence intensity reflect increased Ca^{2+}. Note that the UV flashes are global across the whole file, but appear as white dots on the images due to the position of the spinning disk at the moment of the flash. Video S2 is a differential image series of the same data; the red intensity is proportional to the rate of GCaMP3 fluorescence increase overlaid on the gray scale image. This video is included to better resolve the spatially localized $[Ca^{2+}]_c$ changes, as well as the wave front during Ca^{2+} wave propagation. It should be noted that only the rising phase (not sustained) of each Ca^{2+} transient is observed in the red differential image (Video S2), so this does not show the full duration of Ca^{2+} transients (seen in Video S1).

This switch in $[Ca^{2+}]_c$ oscillation properties between IP_3 uncaging and activation of a PLC-linked GPCR such as VP can be recapitulated in a mathematical model that combines class 1 and class 2 oscillation mechanisms (see Transparent Methods). Specifically, the simulation presented in Figure 5C incorporates positive and negative feedback at the IP_3R using parameters similar to those described previously (Sneyd et al., 2006), which is sufficient to generate $[Ca^{2+}]_c$ oscillations in the presence of incremental sustained elevations of IP_3 (green line). A stepped increase in $[IP_3]$ increases the oscillation frequency with no requirement for dynamic changes of IP_3. Introduction of VP, which activates PLC and allows positive feedback of Ca^{2+} on IP_3 formation, yields much broader $[Ca^{2+}]_c$ oscillations with sustained periods of baseline $[Ca^{2+}]_c$, similar to those observed in Figures 5A and 5B. The model even recapitulates the secondary Ca^{2+} peaks often seen during the falling phase of $[Ca^{2+}]_c$ in the experimental data in response to VP (this is also seen in cells that have not experienced prior IP_3 uncaging events, Figure S2). Importantly, the qualitatively different oscillation patterns shown in Figure 5C are obtained with a single model that allows both intrinsic IP_3R regulation by Ca^{2+} and Ca^{2+} regulation of IP_3 levels in the presence of hormone.

At subcellular resolution, the broad hormone-dependent $[Ca^{2+}]_c$ oscillations in hepatocytes typically propagated starting at the same puff site that was activated during IP_3 uncaging. Following addition of VP, a single broad $[Ca^{2+}]_c$ response with complicated oscillatory behavior was often observed during the transition to baseline-separated $[Ca^{2+}]_c$ oscillations (Figures 5A and 5B). $[Ca^{2+}]_c$ transients generated by uncaging IP_3 had a higher frequency at the puff site (Figure 5E), a narrower spike width (Figure 5F), and a faster rate of $[Ca^{2+}]_c$ rise (Figure 5G) compared with the distal pole of the cell. Hormone-induced Ca^{2+} oscillations had a much greater width (FWHM, Figure 5F), with greater ISI (Figures 5D and 5E), compared with responses generated solely by uncaging IP_3. Unlike the responses generated by IP_3 uncaging, no differences in spike width, ISI, or rate of rise between the puff site and distal regions of the cell were observed with hormone-dependent $[Ca^{2+}]_c$ oscillations. These data show a clear switch in $[Ca^{2+}]_c$ oscillation properties between IP_3 uncaging and stimulation via a PLC-linked GPCR in hepatocytes. Our modeling studies reveal that the ability of hormones to generate all-or-none oscillatory propagating Ca^{2+} waves can be ascribed to the Ca^{2+}-dependent stimulation of PLC, which only occurs with GPCR activation. This positive feedback of Ca^{2+} on PLC ensures that cellular IP_3 levels consistently reach a level that is sufficient to engage the whole

cell during each Ca^{2+} oscillation in the presence of hormone. By contrast, in the absence of hormone there is no stimulation of PLC activity when IP_3 is uncaged, resulting in local responses at the "eager" Ca^{2+} release sites and fast narrow $[Ca^{2+}]_c$ transients that do not reliably propagate throughout the cell.

Discussion

Ca^{2+} oscillation and waves generated by the PLC-linked GPCRs are a major class of Ca^{2+} signals that regulate a host of intracellular processes. In hepatocytes, hormone-induced $[Ca^{2+}]_c$ oscillations regulate cellular metabolism, bile secretion, gene expression, and glucose homeostasis (Amaya and Nathanson, 2013; Bartlett et al., 2014). The hepatocyte was one of the first cell types to be shown to signal through Ca^{2+} oscillations, and these cells remain one of the best examples of frequency-modulated signaling, with a broad frequency response range and long-period baseline-separated $[Ca^{2+}]_c$ transients (Bartlett et al., 2014; Hajnoczky et al., 1995; Rooney et al., 1989; Woods et al., 1986, 1987). The mechanisms that give rise to $[Ca^{2+}]_c$ oscillations have been the topic of much study and discussion, which has been complicated by the existence of two distinct paradigms that have been evidenced in different cellular systems: class 1 oscillations that are essentially intrinsic to the IP_3R and rely on positive and negative feedback effects of Ca^{2+} on the Ca^{2+} release channel (Sneyd et al., 2006, 2017; Thurley and Falcke, 2011) and class 2 oscillations in which Ca^{2+} feedback acts at the level of IP_3 formation and/or breakdown (Dupont and Erneux, 1997; Gaspers et al., 2014; Harootunian et al., 1991; Politi et al., 2006; Sneyd et al., 2006). It has generally been considered that the main determinants dictating the utilization of these mechanisms lie in the cellular complement of Ca^{2+} toolkit components, and that the higher-frequency-intrinsic IP_3R oscillator will tend to dominate in the presence of sufficiently elevated IP_3.

In the present study, we demonstrate the coexistence of both types of oscillatory Ca^{2+} signaling in primary rat hepatocytes and show that in contrast to the IP_3R-level class 1 oscillation mechanism dominating, class 2 mechanisms become important when an agonist is added to activate the GPCR-dependent PLC and elicit IP_3 formation. Moreover, Ca^{2+} oscillations elicited by uncaging IP_3 and those generated by the hormone VP are qualitatively different and generated by distinct mechanisms, but, nevertheless, share components of the same Ca^{2+} toolkit. Both mechanisms can be recapitulated in a single mathematical model without changing any model parameters, but simply allowing for an agonist-dependent formation of IP_3 in a Ca^{2+}-regulated manner. The simplicity of this divergent behavior in a convergent model makes it clear that the same elements of the Ca^{2+} signaling toolkit give rise to the full range of Ca^{2+} signaling in hepatocytes. Thus, at least in the hepatocyte, the class 1 and class 2 oscillation mechanisms are not mutually exclusive, but integrate to give rise to the complex patterns of $[Ca^{2+}]_c$ signals seen in these cells. In a hybrid class 2 model, Ca^{2+} and IP_3 oscillations are co-dependent, and in effect cross-coupled through mutual feedback regulation. Positive Ca^{2+} feedback on PLC ensures that sufficient IP_3 is produced for a global cell-wide $[Ca^{2+}]_c$ response and drives Ca^{2+} release, whereas positive Ca^{2+} feedback on the IP_3R ensures the rapid rising phase of the Ca^{2+} transients. In the context of the "Ca^{2+} toolkit" described by Berridge and others (Berridge et al., 2000; Bootman and Berridge, 1995; Bootman et al., 1997b), the key determinant of this type of Ca^{2+} oscillation is the involvement of $G\alpha_q$-linked GPCRs that engage the Ca^{2+}-sensitive PLCβ enzymes. By contrast, photorelease of caged IP_3 initiates solely class 1 Ca^{2+} oscillations, and whereas this is a non-physiological stimulus, other physiological stimuli that act through IP_3 but do not activate a Ca^{2+}-sensitive PLC could still elicit $[Ca^{2+}]_c$ oscillations through predominantly class 1 mechanisms in hepatocytes, for example, growth factors that signal through PLCγ (Baffy et al., 1992) and agonists that enhance IP_3R activity through, for example, cAMP-dependent phosphorylation (Joseph and Ryan, 1993; Bartlett et al., 2014).

An important characteristic of the $[Ca^{2+}]_c$ oscillations elicited by PLCβ-linked GPCRs is their robustness, both in the temporal domain and in their spatial organization. In the presence of hormones such as VP, Ca^{2+} transients occur with a regular period and relatively little variation of ISI, whereas the Ca^{2+} transients occurring in response to IP_3 uncaging are much more stochastic. This implies a larger contribution from deterministic components under the conditions of hormone stimulation (Thurley et al., 2014), which likely reside in the metabolic steps of IP_3 formation and breakdown. Presumably it is the linked cascade of metabolic steps and Ca^{2+} feedback on these that gives rise to the other notable difference between $[Ca^{2+}]_c$ oscillations induced by IP_3 uncaging and hormone treatment, which is the much greater duration of the Ca^{2+} transients elicited by hormone. These broader $[Ca^{2+}]_c$ transient kinetics are known to be independent of agonist dose, but do show characteristically distinct shapes with different agonists (Bartlett et al., 2014; Green et al., 1993; Rooney et al., 1989).

A potential explanation for the agonist-specific $[Ca^{2+}]_c$ spike shapes is differential modulation of the generation and/or metabolism of IP_3 by distinct GPCRs. An additional component of the G_q-linked PLC pathway is the generation of diacylglycerol and activation of PKC, concurrent with the production of IP_3. Many components of the Ca^{2+} signaling toolkit are substrates for PKC isoforms, and the activity of these kinases could contribute to oscillatory IP_3 production (Nash et al., 2001; Woodring and Garrison, 1997; Bartlett et al., 2015). GPCRs can be phosphorylated by PKC (Nash et al., 2001), which decreases their coupling to G proteins. Consistent with this, we and others have shown that PKC inhibition enhances hormone-induced Ca^{2+} signaling, whereas acute PKC activation with phorbol ester decreases Ca^{2+} oscillation frequency (Bartlett et al., 2015; Sanchez-Bueno et al., 1990). PKC phosphorylation may also modify the activity of IP_3Rs (Matter et al., 1993; Arguin et al., 2007), and thus has the potential to affect the onset or duration of class 1 oscillations. Indeed, we have shown that acute phorbol ester treatment increases the frequency of Ca^{2+} oscillations induced by uncaging IP_3 (Bartlett et al., 2015). However, it is important to note that a PKC feedback mechanism to regulate Ca^{2+} or IP_3 metabolism was not included in the modeling data presented here. Thus, although PKC activity may account for agonist-dependent differences in Ca^{2+} transient dynamics, the only factor required for the switch between class 1 and class 2 oscillations in our model is allowing the Ca^{2+} feedforward activation of PLC (Ca^{2+} and IP_3 cross-coupling).

In addition to the longer duration of the Ca^{2+} transients in the presence of hormones, it is also noteworthy that hormone-induced $[Ca^{2+}]_c$ oscillations sustain much longer periods of baseline $[Ca^{2+}]_c$ between Ca^{2+} transients when compared with IP_3 uncaging. During these periods there is no overt stochastic Ca^{2+} spiking like that seen with IP_3 uncaging. Indeed, hormone-mediated Ca^{2+} signaling not only yields more robust low-frequency oscillations but also appears to suppress stochastic behavior between Ca^{2+} transients. Nevertheless, both IP_3 uncaging and agonist stimulation are associated with dose-dependent increases in $[Ca^{2+}]_c$ oscillation frequency (present work and Bartlett et al., 2014; Bartlett et al., 2015; Gaspers et al., 2014).

The greater robustness of Ca^{2+} signaling with hormones when compared with direct photorelease of IP_3 is also apparent at the spatial level. The $[Ca^{2+}]_c$ oscillations elicited by global uncaging of IP_3 are characterized by local events, which may be sustained in only a small subcellular region, or propagate to other parts of the cell. Even within the same cell, and during a single uncaging event, there can be a mixture of local Ca^{2+} transients, partial propagation, and global Ca^{2+} waves. When they do occur, these global Ca^{2+} signals resulting from IP_3 uncaging vary in their kinetic properties in different parts of the cell, tending to decrease in rates of Ca^{2+} rise and increase in duration from the initial puff site to the distal pole of the cell. By contrast, the $[Ca^{2+}]_c$ oscillations induced by hormone treatment always propagate throughout the cell as a full Ca^{2+} wave, and do so with kinetic properties that are sustained across the cell. Significantly, the hormone-induced $[Ca^{2+}]_c$ oscillations and waves typically originate from the same "eager" Ca^{2+} puff sites that are seen with IP_3 uncaging. These data suggest that the subcellular distribution of IP_3 receptor populations plays a key role in determining the initiation of Ca^{2+} signaling in response to hormones in hepatocytes. However, the combination of the class 1 IP_3R CICR mechanism with the class 2 positive feedforward of Ca^{2+} on PLC to generate sufficient IP_3 yields a more robust signal that ensures that Ca^{2+} release is not spatially restricted in the presence of hormone and gives rise to the properties of propagating intracellular Ca^{2+} waves in hepatocytes. Thus, the combination of two types of interacting Ca^{2+} oscillation mechanisms give rise to a uniform intracellular Ca^{2+} signal with fixed kinetics and relatively low frequency and limits stochastic behavior between Ca^{2+} transients.

Limitations of the Study

In this study we challenge the dogma that different cell types elicit Ca^{2+} oscillations via class 1 or class 2 mechanisms and clearly demonstrate that both phenomena can be observed in primary rat hepatocytes. It is likely that other cell types, particularly those with functional polarization such as epithelial cells, may also generate Ca^{2+} oscillations via a hybrid class 2 mechanism, but examining different cell types was beyond the scope of the present study. A further test of our proposed mechanism would be to demonstrate unequivocally that IP_3 levels oscillate with hormone and not with photorelease of caged IP_3. However, it was not possible to make single-cell IP_3 measurements during IP_3 uncaging and cytosolic Ca^{2+} recording. We and others have shown previously that hormone-induced oscillations in IP_3 occur concurrently with Ca^{2+} oscillations using Förster resonance energy transfer (FRET)-based IP_3 sensors (Gaspers et al., 2014; Tanimura et al., 2009). However, combining flash photolysis of caged IP_3 with detection of IP_3 with FRET probes is technically challenging, because the UV excitation used for uncaging can quench the FRET fluorophore,

and the required blue light excitation may elicit uncontrolled IP_3 uncaging. As an alternative approach we utilized an IP_3 buffer to perturb IP_3 dynamics and demonstrated that fast Ca^{2+} oscillations still occur when IP_3 is photoreleased in the presence of IP_3 buffering (Figure 2), whereas hormone-induced Ca^{2+} oscillations are supressed by the expression of the IP_3 buffer (Gaspers et al., 2014).

SUPPLEMENTAL INFORMATION

Supplemental Information can be found online at https://doi.org/10.1016/j.isci.2020.101062.

METHODS

All methods can be found in the accompanying Transparent Methods supplemental file.

ACKNOWLEDGMENTS

GCaMP3 was a gift from Loren Looger (Addgene plasmid #22692). R-GECO-1 was a gift from Robert Campbell (Addgene plasmid #32444). GCaMP3 and R-GECO-1 were acquired with an MTA between Addgene and Rutgers-NJMS. This work was supported by the Thomas P. Infusion Endowed Chair and NIH R01DK078019 (to A.P.T), NIH R01DE019245-11 (to J.S.), and the University of Auckland Doctoral Scholarship (I.C.).

AUTHOR CONTRIBUTIONS

P.J.B., A.P.T, and J.S. designed the research. P.J.B. and I.C. performed the research. P.J.B. and I.C. analyzed the data. P.J.B. and A.P.T. wrote the manuscript.

DECLARATION OF INTERESTS

The authors declare no competing interests.

Received: March 15, 2019
Revised: December 11, 2019
Accepted: April 9, 2020
Published: May 22, 2020

REFERENCES

Akerboom, J., Carreras Calderón, N., Tian, L., Wabnig, S., Prigge, M., Tolö, J., Gordus, A., Orger, M.B., Severi, K.E., Macklin, J.J., et al. (2013). Genetically encoded calcium indicators for multi-color neural activity imaging and combination with optogenetics. Front. Mol. Neurosci. *6*, 2.

Amaya, M.J., and Nathanson, M.H. (2013). Calcium Signaling in the Liver. Comprehensive Physiology (John Wiley & Sons, Inc).

Arguin, G., Regimbald-Dumas, Y., Fregeau, M.-O., Caron, A.Z., and Guillemette, G. (2007). Protein kinase C phosphorylates the inositol 1,4,5-trisphosphate receptor type 2 and decreases the mobilization of Ca2+in pancreatoma AR4-2J cells. J. Endocrinol. *192*, 659–668.

Arruda, A.P., and Hotamisligil, G.S. (2015). Calcium homeostasis and organelle function in the pathogenesis of obesity and diabetes. Cell Metab. *22*, 381–397.

Baffy, G., Yang, L., Michalopoulos, G.K., and Williamson, J.R. (1992). Hepatocyte growth factor induces calcium mobilization and inositol phosphate production in rat hepatocytes. J. Cell Physiol. *153*, 332–339.

Bartlett, P.J., Antony, A.N., Agarwal, A., Hilly, M., Prince, V.L., Combettes, L., Hoek, J.B., and Gaspers, L.D. (2017). Chronic alcohol feeding potentiates hormone-induced calcium signalling in hepatocytes. J. Physiol. *595*, 3143–3164.

Bartlett, P.J., Gaspers, L.D., Pierobon, N., and Thomas, A.P. (2014). Calcium-dependent regulation of glucose homeostasis in the liver. Cell Calcium *55*, 306–316.

Bartlett, P.J., Metzger, W., Gaspers, L.D., and Thomas, A.P. (2015). Differential regulation of multiple steps in inositol 1,4,5- trisphosphate signaling by protein kinase C shapes hormone-stimulated Ca2+ oscillations. J. Biol. Chem. *290*, 18519–18533.

Berridge, M.J. (2016). The inositol trisphosphate/calcium signaling pathway in health and disease. Physiol. Rev. *96*, 1261–1296.

Berridge, M.J. (2017). Calcium signalling in health and disease. Biochem. Biophys. Res. Commun. *485*, 5.

Berridge, M.J., Lipp, P., and Bootman, M.D. (2000). The versatility and universality of calcium signalling. Nat. Rev. Mol. Cell Biol. *1*, 11–21.

Bezprozvanny, L., Watras, J., and Ehrlich, B.E. (1991). Bell-shaped calcium-response curves of Ins(l,4,5)P3- and calcium-gated channels from endoplasmic reticulum of cerebellum. Nature *351*, 751–754.

Bootman, M., Niggli, E., Berridge, M., and Lipp, P. (1997a). Imaging the hierarchical Ca2+ signalling system in HeLa cells. J. Physiol. *499* (Pt 2), 307–314.

Bootman, M.D., and Berridge, M.J. (1995). The elemental principles of calcium signaling. Cell *83*, 675–678.

Bootman, M.D., Berridge, M.J., and Lipp, P. (1997b). Cooking with calcium: the recipes for composing global signals from elementary events. Cell *91*, 367–373.

De Young, G.W., and Keizer, J. (1992). A single-pool inositol 1,4,5-trisphosphate-receptor-based model for agonist-stimulated oscillations in Ca2+ concentration. Proc. Natl. Acad. Sci. U S A *89*, 9895–9899.

Dupont, G., and Erneux, C. (1997). Simulations of the effects of inositol 1,4,5-trisphosphate 3-kinase and 5-phosphatase activities on Ca2+ oscillations. Cell Calcium *22*, 321–331.

Dupont, G., Houart, G., and de Koninck, P. (2003). Sensitivity of CaM kinase II to the frequency of

Ca2+ oscillations: a simple model. Cell Calcium *34*, 485–497.

Gaspers, L.D., Bartlett, P.J., Politi, A., Burnett, P., Metzger, W., Johnston, J., Joseph, S.K., Hofer, T., and Thomas, A.P. (2014). Hormone-induced calcium oscillations depend on cross-coupling with inositol 1,4,5-trisphosphate oscillations. Cell Rep. *9*, 1209–1218.

Gaspers, L.D., Pierobon, N., and Thomas, A.P. (2019). Intercellular calcium waves integrate hormonal control of glucose output in the intact liver. J. Physiol. *597*, 2867–2885.

Gaspers, L.D., and Thomas, A.P. (2005). Calcium signaling in liver. Cell Calcium *38*, 329–342.

Green, A.K., Dixon, C.J., Mclennan, A.G., Cobbold, P.H., and Fisher, M.J. (1993). Adenine dinucleotide-mediated cytosolic free Ca2+ oscillations in single hepatocytes. FEBS Lett. *322*, 197–200.

Hajnoczky, G., Robb-Gaspers, L.D., Seitz, M.B., and Thomas, A.P. (1995). Decoding of cytosolic calcium oscillations in the mitochondria. Cell *82*, 415–424.

Harootunian, A.T., Kao, J.P., Paranjape, S., Adams, S.R., Potter, B.V., and Tsien, R.Y. (1991). Cytosolic Ca2+ oscillations in REF52 fibroblasts: Ca(2+)-stimulated IP3 production or voltage-dependent Ca2+ channels as key positive feedback elements. Cell Calcium *12*, 153–164.

Hernandez, E., Leite, M.F., Guerra, M.T., Kruglov, E.A., Bruna-Romero, O., Rodrigues, M.A., Gomes, D.A., Giordano, F.J., Dranoff, J.A., and Nathanson, M.H. (2007). The spatial distribution of inositol 1,4,5-trisphosphate receptor isoforms shapes Ca2+ waves. J. Biol. Chem. *282*, 10057–10067.

Joseph, S.K., and Ryan, S.V. (1993). Phosphorylation of the inositol trisphosphate receptor in isolated rat hepatocytes. J. Biol. Chem. *268*, 23059–23065.

Kummer, U., Olsen, L.F., Dixon, C.J., Green, A.K., Bornberg-Bauer, E., and Baier, G. (2000). Switching from simple to complex oscillations in calcium signaling. Biophysical J. *79*, 1188–1195.

Lock, J.T., Smith, I.F., and Parker, I. (2017). Comparison of Ca2+ puffs evoked by extracellular agonists and photoreleased IP3. Cell Calcium *63*, 43–47.

Marchant, J., Callamaras, N., and Parker, I. (1999). Initiation of IP(3)-mediated Ca(2+) waves in Xenopus oocytes. EMBO J. *18*, 5285–5299.

Marchant, J.S., and Parker, I. (2001). Role of elementary Ca(2+) puffs in generating repetitive Ca(2+) oscillations. EMBO J. *20*, 65–76.

Matter, N., Ritz, M.F., Freyermuth, S., Rogue, P., and Malviya, A.N. (1993). Stimulation of nuclear protein kinase C leads to phosphorylation of nuclear inositol 1,4,5-trisphosphate receptor and accelerated calcium release by inositol 1,4,5-trisphosphate from isolated rat liver nuclei. J. Biol. Chem. *268*, 732–736.

Meyer, T., and Stryer, L. (1988). Molecular model for receptor-stimulated calcium spiking. Proc. Natl. Acad. Sci. U S A *85*, 5051–5055.

Nagata, J., Guerra, M.T., Shugrue, C.A., Gomes, D.A., Nagata, N., and Nathanson, M.H. (2007). Lipid rafts establish calcium waves in hepatocytes. Gastroenterology *133*, 256–267.

Nash, M.S., Young, K.W., Challiss, R.A., and Nahorski, S.R. (2001). Intracellular signalling. Receptor-specific messenger oscillations. Nature *413*, 381–382.

Politi, A., Gaspers, L.D., Thomas, A.P., and Hofer, T. (2006). Models of IP3 and Ca2+ oscillations: frequency encoding and identification of underlying feedbacks. Biophys. J. *90*, 3120–3133.

Rooney, T.A., Sass, E.J., and Thomas, A.P. (1989). Characterization of cytosolic calcium oscillations induced by phenylephrine and vasopressin in single fura-2-loaded hepatocytes. J. Biol. Chem. *264*, 17131–17141.

Rooney, T.A., Sass, E.J., and Thomas, A.P. (1990). Agonist-induced cytosolic calcium oscillations originate from a specific locus in single hepatocytes. J. Biol. Chem. *265*, 10792–10796.

Salazar, C., Politi, A.Z., and Hofer, T. (2008). Decoding of calcium oscillations by phosphorylation cycles: analytic results. Biophys. J. *94*, 1203–1215.

Sanchez-Bueno, A., Dixon, C.J., Woods, N.M., Cuthbertson, K.S., and Cobbold, P.H. (1990). Inhibitors of protein kinase C prolong the falling phase of each free-calcium transient in a hormone-stimulated hepatocyte. Biochem. J. *268*, 627–632.

Smith, I.F., Wiltgen, S.M., and Parker, I. (2009). Localization of puff sites adjacent to the plasma membrane: functional and spatial characterization of Ca2+ signaling in SH-SY5Y cells utilizing membrane-permeant caged IP3. Cell Calcium *45*, 65–76.

Sneyd, J., Han, J.M., Wang, L., Chen, J., Yang, X., Tanimura, A., Sanderson, M.J., Kirk, V., and Yule, D.I. (2017). On the dynamical structure of calcium oscillations. Proc. Natl. Acad. Sci. U S A *114*, 1456–1461.

Sneyd, J., Tsaneva-Atanasova, K., Reznikov, V., Bai, Y., Sanderson, M.J., and Yule, D.I. (2006). A method for determining the dependence of calcium oscillations on inositol trisphosphate oscillations. Proc. Natl. Acad. Sci. U S A *103*, 1675–1680.

Tanimura, A., Morita, T., Nezu, A., Shitara, A., Hashimoto, N., and Tojyo, Y. (2009). Use of fluorescence resonance energy transfer-based biosensors for the quantitative analysis of inositol 1,4,5-trisphosphate dynamics in calcium oscillations. J. Biol. Chem. *284*, 8910–8917.

Thomas, A.P., Bird, G.S., Hajnoczky, G., Robb-Gaspers, L.D., and Putney, J.W., JR. (1996). Spatial and temporal aspects of cellular calcium signaling. FASEB J. *10*, 1505–1517.

Thomas, A.P., Renard, D.C., and Rooney, T.A. (1991). Spatial and temporal organization of calcium signalling in hepatocytes. Cell Calcium *12*, 111–126.

Thomas, A.P., and Robb-Gaspers, L.D. (1996). Subcellular and multicellular organization of calcium signaling in liver. In Microscopy and Microanalysis 1996, G.W. Bailey, J.M. Corbett, R.V.M. Dimlich, J.R. Michael, and N.J. Zaluzec, eds. (San Francisco Press, Inc), pp. 736–737.

Thomas, D., Lipp, P., Tovey, S.C., Berridge, M.J., LI, W., Tsien, R.Y., and Bootman, M.D. (2000). Microscopic properties of elementary Ca2+ release sites in non-excitable cells. Curr. Biol. *10*, 8–15.

Thurley, K., and Falcke, M. (2011). Derivation of Ca2+ signals from puff properties reveals that pathway function is robust against cell variability but sensitive for control. Proc. Natl. Acad. Sci. U S A *108*, 427–432.

Thurley, K., Tovey, S.C., Moenke, G., Prince, V.L., Meena, A., Thomas, A.P., Skupin, A., Taylor, C.W., and Falcke, M. (2014). Reliable encoding of stimulus intensities within random sequences of intracellular Ca2+ spikes. Sci. Signal. *7*, ra59.

Tovey, S.C., de Smet, P., Lipp, P., Thomas, D., Young, K.W., Missiaen, L., de Smedt, H., Parys, J.B., Berridge, M.J., Thuring, J., et al. (2001). Calcium puffs are generic $InsP_3$-activated elementary calcium signals and are downregulated by prolonged hormonal stimulation to inhibit cellular calcium responses. J. Cell Sci. *114*, 3979.

Woodring, P.J., and Garrison, J.C. (1997). Expression, purification, and regulation of two isoforms of the inositol 1,4,5-trisphosphate 3-kinase. J. Biol. Chem. *272*, 30447–30454.

Woods, N.M., Cuthbertson, K.S., and Cobbold, P.H. (1986). Repetitive transient rises in cytoplasmic free calcium in hormone-stimulated hepatocytes. Nature *319*, 600–602.

Woods, N.M., Cuthbertson, K.S.R., and Cobbold, P.H. (1987). Agonist-induced oscillations in cytoplasmic free calcium concentration in single rat hepatocytes. Cell Calcium *8*, 79–100.

iScience, Volume *23*

Supplemental Information

IP_3-Dependent Ca^{2+} Oscillations Switch into a Dual Oscillator Mechanism in the Presence of PLC-Linked Hormones

Paula J. Bartlett, Ielyaas Cloete, James Sneyd, and Andrew P. Thomas

Figure S1

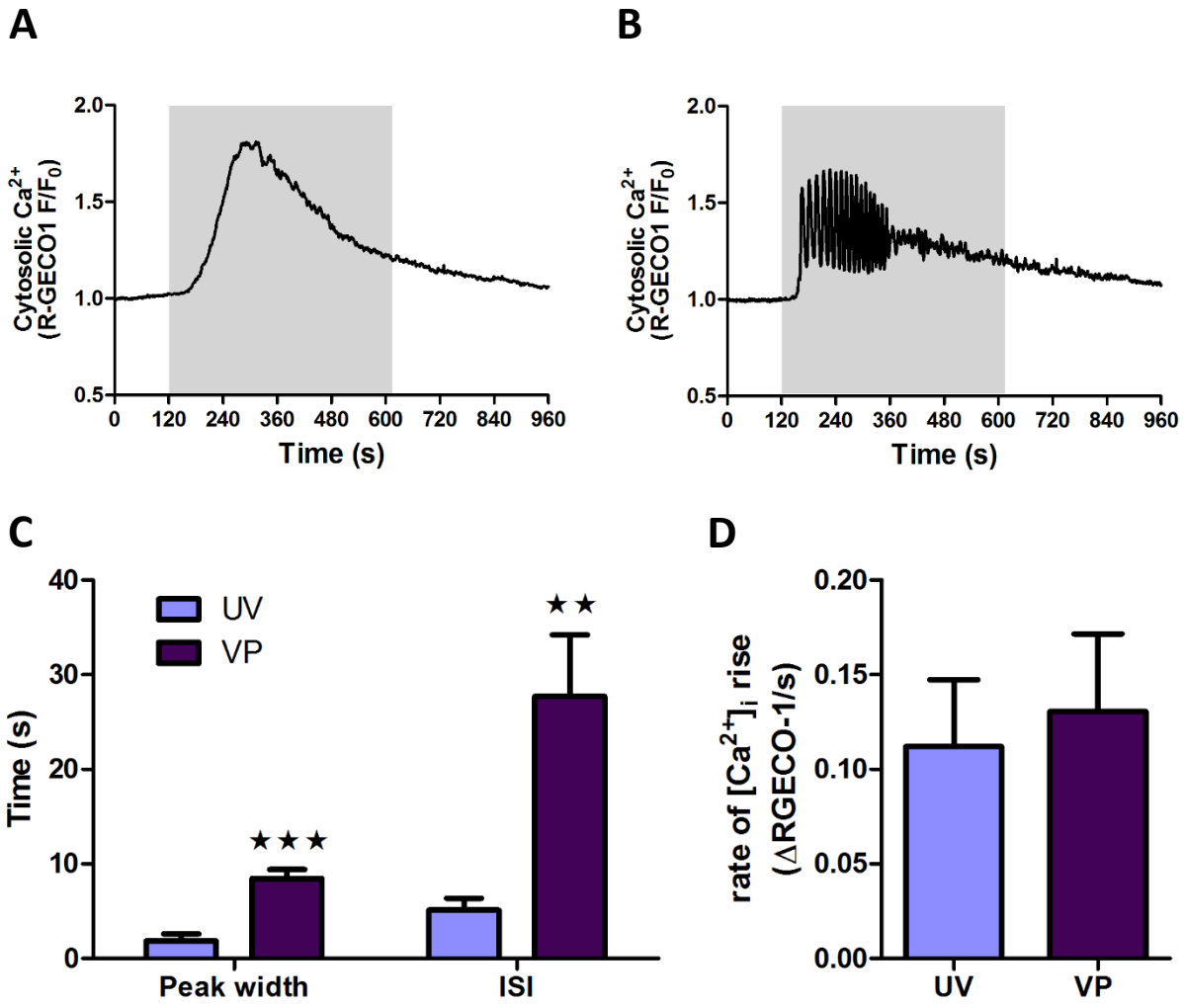

Figure S1. Related to Figure 2. Slow continuous release of caged IP_3 elicits $[Ca^{2+}]_c$ oscillations. Hepatocytes were transfected with RGECO1, cultured overnight and then loaded with caged IP_3 (2 μM; 1 h). Representative traces of slow monophasic (**A**) and oscillatory (**B**) $[Ca^{2+}]_c$ increases (22 cells exhibited oscillatory behavior; total of 45 cells; n=6 experiments). Gray area shows duration of slow IP_3 uncaging with low-intensity UV illumination (50 ms exposures from microscope xenon lamp at 2 Hz). Panels **C** and **D** show data only from oscillating cells. Peak width (FWHM) and ISI of $[Ca^{2+}]_c$ oscillations induced by photorelease of caged IP_3 were shorter than with VP (5 nM added subsequently to the same cells) (**C**), but there was no difference in the rate of $[Ca^{2+}]_c$ rise (**D**). Data are mean±SEM (10 cells from 6 independent experiments). ** $p<0.01$, ***$p<0.001$ paired Student's t-test.

Figure S2

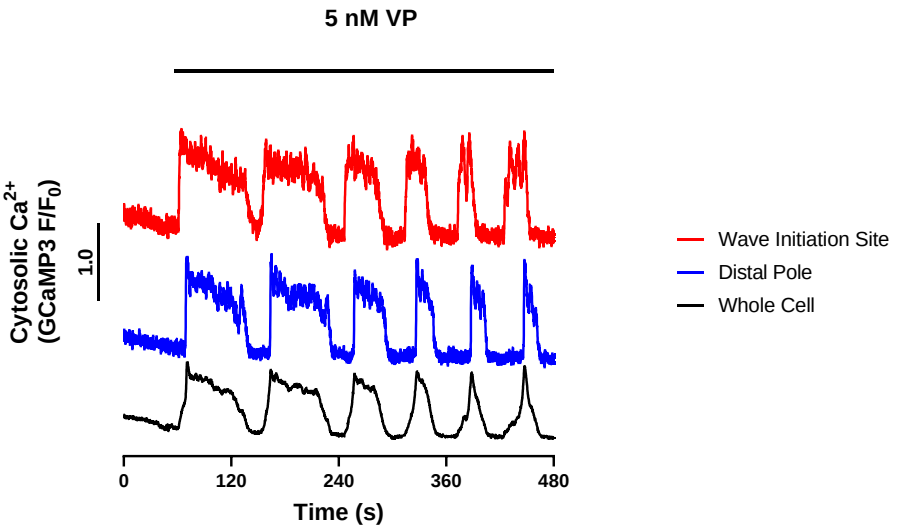

Figure S2. Related to Figure 3. Vasopressin-induced Ca^{2+} oscillations in naïve cells. Hepatocytes were transfected with GCaMP3, cultured overnight and then loaded with caged IP_3 (2 μM; 1 h) for comparison with uncaging studies, but were not exposed to UV light. Traces of $[Ca^{2+}]_c$ from regions of interest at the Ca^{2+} wave initiation site, the distal pole of the cell and the whole cell are shown. Asynchronous local fluctuations in Ca^{2+} during the cell-wide oscillations are not as apparent when the integrated Ca^{2+} response of the whole cell is plotted. Similar VP responses with spatial heterogeneity were observed in 4 independent experiments.

Figure S3

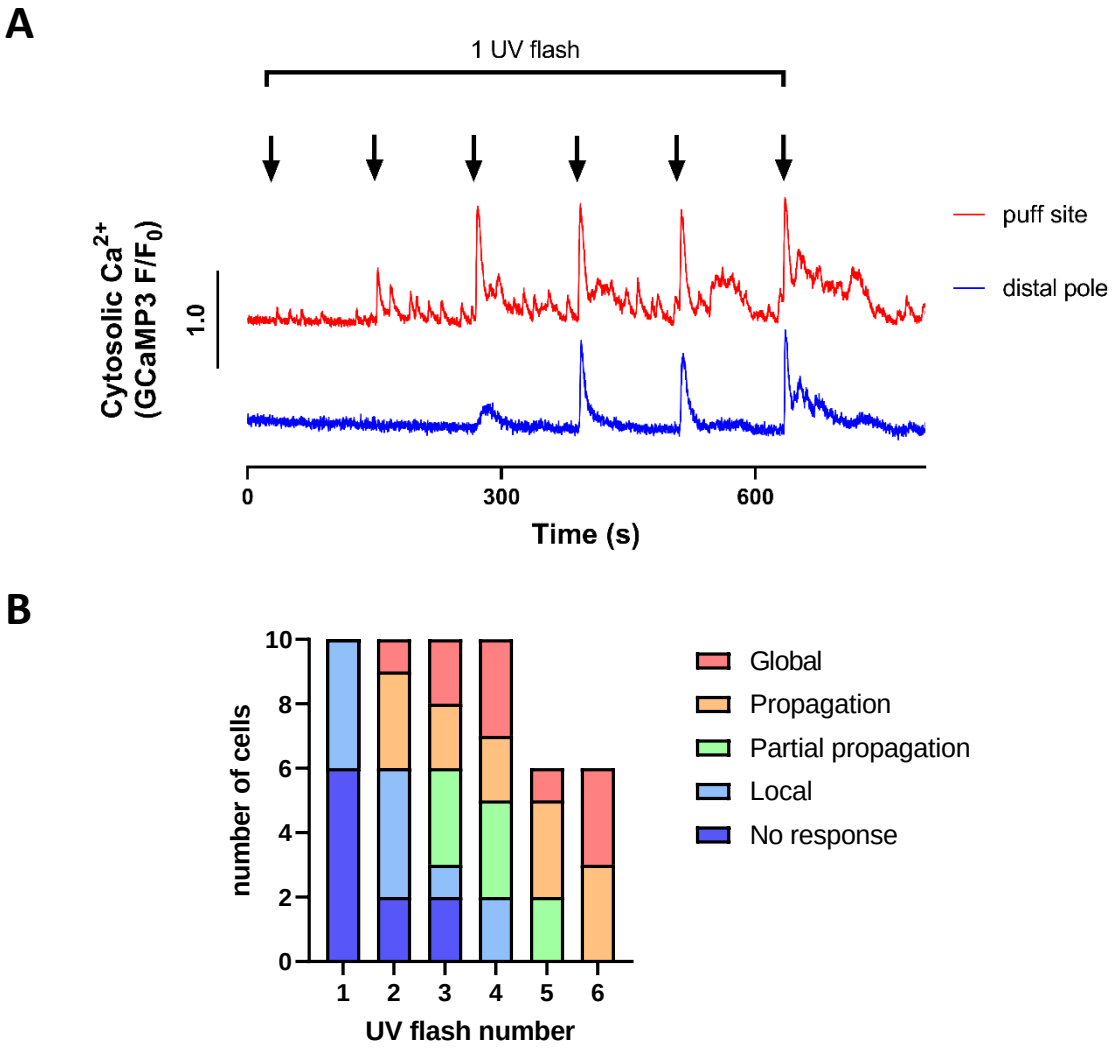

Figure S3. Related to Figure 5. Periodic release of caged IP_3 does recapitulate VP-induced Ca^{2+} oscillations.

Hepatocytes were transfected with GCaMP3, cultured overnight and then loaded with caged IP_3 (2 μM; 1 h). Hepatocytes were exposed to single UV flashes at 2 min intervals. **A:** Traces of $[Ca^{2+}]_c$ from regions of interest at the puff site and the distal pole of the cell (representative of three independent experiments). **B:** Summary data to show proportion of cells responding to each individual UV pulse with ***no response***, ***local*** responses at the puff site, ***partial propagation*** with intermittent Ca^{2+} waves, ***propagation*** of Ca^{2+} waves consistently across the cell, and ***global*** Ca^{2+} responses across the entire cell (summary of 10 cells from 3 independent experiments, note 1 experiment only contained 4 UV pulse events).

Transparent Methods

Primary cell culture. Isolated hepatocytes were prepared by collagenase perfusion of livers obtained from male Sprague-Dawley rats. Cells were transfected with GCaMP3 (Tian et al., 2009) R-GECO1 (Zhao et al., 2011), GFP or GFP-LBD (Gaspers et al., 2014) cDNA using nucleofection (Alonza) then maintained in Williams E media for 16-24 h, as described previously (Rooney et al., 1989). Animal studies were approved by the Institutional Animal Care and Use Committee at Rutgers, New Jersey Medical School.

Flash Photorelease of caged IP_3.

Overnight cultured hepatocytes were incubated in medium composed of (in mM): 121 NaCl, 25 HEPES, 5 $NaHCO_3$, 4.7 KCl, 1.2 KH_2PO_4, 1.2 $MgSO_4$, 1.3 $CaCl_2$, 5.5 glucose, Where required, cells were loaded with the membrane permeant form of caged IP_3 (2 μM, D-2, 3-*O*-isopropylidene-6-*O*-(2-nitro-4,5-dimethoxy)benzyl-*myo*-inositol 1,4,5-trisphosphate-hexakis(propionoxymethyl) ester; Sichem GmbH) for 1 h at room temperature. Cells were transferred to the microscope chamber of a spinning disk confocal microscope. GCaMP3 images (excitation, 488 nm; emission 510 nm long band pass filter) were acquired at 10 Hz. Photorelease of caged IP_3 was achieved by light pulses from a nitrogen charged UV laser (Photon Technology International). The cell permeant caged IP_3 is synthesized with the 2- and 3-hydroxyl groups of myo-inositol protected by an isopropylidene group to ensure that the phosphate groups remain in the 1,4 and 5 positions (Dakin and Li, 2007). Of note, once released from the cage this modified form of IP_3 is metabolized at a slower rate, in the order of minutes, compared to natural IP_3 which is metabolized in seconds (Dakin and Li, 2007). Cell viability was assessed by the addition of maximal hormone concentrations at the end of each experiment. Only cells responsive to hormone stimulation are included in the presented data.

Slow photorelease of caged IP_3

Coverslips were prepared as described above and transferred to the stage of an epifluorescence microscope coupled to a Xeon lamp with high speed wave length switching capabilities (DG4 Sutter). Cells expressing recombinant proteins were selected by screening for GFP fluorescence (excitation 488 nm, emission 525 nm). R-GECO1 images (excitation 548 nM, emission 600 nm)

were acquired at 2 Hz. Continuous photorelease of caged IP_3 was achieved with 50 ms exposure to 380 nm light at 2 Hz.

Mathematical model

We model only the apical region of the hepatocyte which is assumed to be spatially homogeneous. Let $c = [\mathrm{Ca}^{2+}], c_e = [\mathrm{Ca}^{2+}]_{ER}, p = [\mathrm{IP}_3], c_t = c + \gamma c_e$, where γ is the ratio of the ER to the cytoplasmic volume. Also, let *h* be a variable that controls the rate at which IPR can be activated by Ca^{2+}, as described in (Sneyd et al., 2017). Then, conservation gives $dc/dt = J_{\mathrm{IPR}} - J_{\mathrm{serca}} + \delta(J_{\mathrm{in}} - J_{\mathrm{pm}}), dc_t/dt = \delta(J_{\mathrm{in}} - J_{\mathrm{pm}}), dp/dt = \tau_p(p_s - p)$, while the dynamics of the IPR result in the equation $\tau_h \, dh/dt = h_\infty - h$. Expressions and notation for each flux are as in (Sneyd et al., 2017), the only differences being the parameters $t_{max} = 80$, $K_t = 0.09$, $K_f = 4$, $\overline{K} =$ 1.5e-5, $V_{pm} = 0.07$, $a_0 = 0.004$, $\square_1 = 0.01$, $K_{ce} = 14$, $d = 2.5$, $k_b = 0.4$ (all units the same as in (Sneyd et al., 2017)), and in the expression for p_s. In the absence of VP, $p_s = 0$, while, in the presence of VP, $p_s = V_{PLC}c^2/(K_{PLC}^2 + c^2)$, where V_{PLC}=0.16 mM/s, K_{PLC}=0.1 mM.

Supplemental References

DAKIN, K. & LI, W.-H. 2007. Cell membrane permeable esters of d-myo-inositol 1,4,5-trisphosphate. *Cell Calcium,* 42**,** 291-301.

GASPERS, L. D., BARTLETT, P. J., POLITI, A., BURNETT, P., METZGER, W., JOHNSTON, J., JOSEPH, S. K., HOFER, T. & THOMAS, A. P. 2014. Hormone-induced calcium oscillations depend on cross-coupling with inositol 1,4,5-trisphosphate oscillations. *Cell Rep,* 9**,** 1209-18.

ROONEY, T. A., SASS, E. J. & THOMAS, A. P. 1989. Characterization of cytosolic calcium oscillations induced by phenylephrine and vasopressin in single fura-2-loaded hepatocytes. *The Journal of biological chemistry,* 264**,** 17131-41.

SNEYD, J., HAN, J. M., WANG, L., CHEN, J., YANG, X., TANIMURA, A., SANDERSON, M. J., KIRK, V. & YULE, D. I. 2017. On the dynamical structure of calcium oscillations. *Proceedings of the National Academy of Sciences of the United States of America,* 114**,** 1456-1461.

TIAN, L., HIRES, S. A., MAO, T., HUBER, D., CHIAPPE, M. E., CHALASANI, S. H., PETREANU, L., AKERBOOM, J., MCKINNEY, S. A., SCHREITER, E. R., BARGMANN, C. I., JAYARAMAN, V., SVOBODA, K. & LOOGER, L. L. 2009. Imaging neural activity in worms, flies and mice with improved GCaMP calcium indicators. *Nature methods,* 6**,** 875-881.

ZHAO, Y., ARAKI, S., WU, J., TERAMOTO, T., CHANG, Y. F., NAKANO, M., ABDELFATTAH, A. S., FUJIWARA, M., ISHIHARA, T., NAGAI, T. & CAMPBELL, R. E. 2011. An expanded palette of genetically encoded Ca(2)(+) indicators. *Science,* 333**,** 1888-91.